International Journal of Thermal Sciences 49 (2010) 1156–1164

Contents lists available at ScienceDirect

International Journal of Thermal Sciences

journal homepage: www.elsevier.com/locate/ijts

Boiling characteristics of carbon nanotube suspensions under sub-atmospheric pressures

Zhen-Hua Liu*, Xue-Fei Yang, Jian-Guo Xiong

School of Mechanical Engineering, Shanghai Jiaotong University, 800 Dongchuan Road, Shanghai 200240, PR China

ARTICLE INFO

Article history:
Received 14 July 2009
Received in revised form
15 December 2009
Accepted 27 January 2010
Available online 11 March 2010

Keywords:
Boiling
Heat transfer enhancement
Nanofluid
Carbon nanotube
Contact angle

ABSTRACT

An experimental study was performed to understand the pool boiling heat transfer of deionized water-based carbon nanotube (CNT) suspensions on a flat copper surface under atmospheric and sub-atmospheric pressures. Experimental results indicate that the addition of CNT in the base liquid can apparently enhance both the heat transfer coefficient (HTC) and the critical heat flux (CHF). The pressure has great impacts on both the HTC and the CHF enhancement of CNT suspensions and the both increase significantly with the decrease of the pressure. The CNT mass concentration of CNT suspensions also has strong influences on both the HTC and the CHF of CNT suspensions and there exists an optimal CNT mass concentration corresponding to the maximum heat transfer enhancement. Besides, the effects of the surface characteristics of the heated surface on both the HTC and the CHF of CNT suspensions were also investigated.

1. Introduction

Nanofluid as a new kind of functional fluid has many unique characteristics. It's an innovative research to use nanofluid technology in traditional thermal engineering fields. A number of studies have been carried out to understand and describe the larruping behaviors of nanofluid, such as its thermal conductivity under the static conditions [1–6], the convective heat transfer associated with fluid flow and heat transfer phenomenon [7–14] and phase change heat transfer [15–28]. Most of the investigations indicated that the addition of nanoparticles could increase the effective thermal conductivity with the increase of the nanoparticle concentration. Therefore, studies concerning nanofluids focused mainly on the single-phase heat transfer.

Compared with the research efforts in thermal conductivity and forced convective heat transfer, relatively fewer studies have been carried out on pool boiling heat transfer. Das et al. [15] firstly conducted an investigation on the pool boiling of the deionized water-based Al_2O_3 nanoparticle suspension on a horizontal tubular heater having a diameter of 20 mm with different surface roughness at atmospheric pressure. The heat flux ranged from 2×10^4 W/m^2 to 1.2×10^5 W/m^2. No surfactant was added into suspensions. It was found that the nanoparticle suspensions have poor heat transfer compared with pure deionized water. Surface roughness could also greatly affect the nucleation superheat. The required superheat for a smooth surface was usually higher than that for a rough surface. When the volume concentration of nanoparticles was higher than 0.1%, the effect was well-regulated in their experimental conditions, and the superheat for high concentration nanoparticle suspensions was higher than that for low concentration nanoparticle suspensions at a specified heat flux. The subsidence of nanoparticles was considered as the main reason for the increase of superheat.

Vassallo and co-workers [16] carried out a pool boiling experiment of deionized water-based silica nanoparticle suspensions on a horizontal NiCr wire at atmospheric pressure. No surfactant was added into suspensions. A remarkable increase in critical heat flux (CHF) was observed compared with pure deionized water. But, no appreciable differences in the boiling heat transfer were found for the heat flux less than the CHF.

Bang and Cheng [17] conducted an investigation on the pool boiling of deionized water-based Al_2O_3 nanoparticle suspensions on a plain heating plate at atmospheric pressure. The test surface is a 4×100 mm^2 rectangle with a depth of 1.9 mm. No surfactant was added into suspensions in their experiment. It was found that the boiling heat transfer characteristics of the nanoparticle suspensions were poor compared with pure deionized water in the nucleate boiling region. For the horizontal test surface, however, the CHF increased by 32% compared with the pure deionized water case. These were due to the changes of the surface characteristics by the deposition of nanoparticles on the heated surface.

* Corresponding author. Tel.: +86 21 34206568.
E-mail address: liuzhenh@sjtu.edu.cn (Z.-H. Liu).

1290-0729/$ – see front matter © 2010 Elsevier Masson SAS. All rights reserved.
doi:10.1016/j.ijthermalsci.2010.01.023

Nomenclature

g	gravity acceleration (m/s^2)
c_p	specific heat (kJ/kg/K)
h	heat transfer coefficient (W/K/m^2)
h_{fg}	latent heat of evaporation (J/kg)
p	pressure (Pa)
P_r	Prandtl number
q	heat flux (W/m^2)
q''	critical heat flux (W/m^2)
T	temperature (°C)
w	CNT mass concentration of CNT suspensions(wt%)
λ	thermal conductivity (W/m/K)
η	kinematic viscosity (m^2/s)
σ	surface tension (N/m)
ρ	density (kg/m^3)
β	contact angle (°)
φ	volume fraction (%)

Subscripts

0	base liquid (deionized water)
l	liquid
v	vapor
s	CNT suspension
P	nanoparticles

You and Kim [19] carried out an investigation on the CHF of deionized water-Al_2O_3 nanoparticles-suspensions in a pool boiling experiment with a flat square heater at the pressure of 28.9 kPa. The experimental results demonstrated that the CHF increased dramatically two times compared with pure deionized water. However, the nucleate boiling heat transfer coefficients appeared to be about the same.

Das, Narayan and Anoop et al. [26–28] investigated effects of various nanoparticle parameters such as orientation interaction, particle size relative to roughness on pool boiling heat transfer of nanoparticle suspensions, and discussed the Mechanism of enhancement/deterioration of boiling heat transfer using stable nanoparticle suspensions.

Recently, Kim and co-workers [29–31] investigated the surface wettability of nanofluids during pool boiling and its effect on CHF. The working liquids were deionized water-based alumina, zirconia and silica nanofluids. A porous layer of nanoparticles formed on the heated surface during nucleate boiling. This layer significantly improved the surface wettability. They established a nexus between CHF enhancement and surface wettability and considered that the mechanism of CHF enhancement in nanofluids is due to the increase of the heated surface wettability.

Based on the previous researches, the present study investigated the pool boiling characteristics at atmospheric and sub-atmospheric pressures. Carbon nanotube (CNT) suspensions were used as the working liquids. The study mainly focused on the effects of the operating pressure, the mass concentration and the contact angle of the heated surface on the boiling heat transfer of CNT suspensions. In particular, the boiling characteristics of CNT suspensions under sub-atmospheric pressures were tested and discussed.

2. Experimental apparatus and procedures

In the present study, carbon nanotube (CNT) suspensions consisting of deionized deionized water and multi-wall carbon nanotubes were applied as the working liquids. The carbon nanotubes have an average diameter of 15 nm and a length range of 5–15 μm. Fig. 1 shows a TEM photograph of the CNT suspension with its mass concentration of 1.0 wt%. The photograph shows a good dispersing state of CNT in deionized deionized water.

During the preparation stage of the CNT suspension, the CNTs were firstly added in an alkali/deionized water mixture. The CNT–alkali/deionized water mixture then was oscillated continuously for about 10 h in an ultrasonic deionized water bath to break up the self-winding structure of the CNTs and make the steady CNT suspension. Later, the nitric acid was added into the CNT suspension and the PH value was adjusted to a constant of 6.5. Finally, the CNT suspension was again oscillated continuously for about 2 h and was then hold in a tank. Before the boiling experiment, the suspension was oscillated again for about 2 h, so three stages of oscillation were used in the whole preparation of the CNT suspension. The mass concentration of the CNT in the present experiment was in the range of 0.5 wt% to 4.0 wt%. The relationship of the mass concentration of nanoparticles and the volume concentration could be conducted as below,

$$\frac{1-w}{w}\frac{\rho_P}{\rho_0} = \frac{1-\varphi}{\varphi} \tag{1}$$

The density and the specific heat of the suspensions were calculated as:

$$\rho_s = \left(\frac{1-w}{\rho_0} + \frac{w}{\rho_P}\right)^{-1} \tag{2}$$

$$c_{p,s} = c_{p,p}\cdot\varphi + c_{p,0}\cdot(1-\varphi) \tag{3}$$

Fig. 2 shows the schematic of the experimental apparatus. It mainly consisted of a test chamber, a heating copper bar, a condensing system, a data acquisition system, a power supply, a vacuum pumping unit and a liquid-filling device. The space between the copper bar and the test box made of stainless steel was filled by asbestos for thermal insulation. A cartridge electric heater was vertically inserted into the copper bar as the main heater. Another electric heater wrapped over the copper bar was used as the auxiliary heater. A cooling deionized water flow system was used to cool the top of the test chamber and condense the vapor in the test chamber. Working liquid was charged into the test chamber and boiled on the top surface of the copper bar. The depth of the working liquid was fixed at 20 mm.

In the test, in order to compensate the heat losses from the copper bar, the power of the auxiliary heater was carefully adjusted to surely make the input power from main electrical heater equaling to the measured output power on the heated surface.

Fig. 3 gives out the schematic configuration of the upper part of the copper bar and the heated surface. The upper part of the copper bar was a cube and the dimension of the top surface was 40 mm × 40 mm. Six thermocouples having a diameter of 1.0 mm were inserted horizontally into the copper bar. They were divided as two teams; one team including tree thermocouples was use to measure the temperature distribution at the central axis of the copper bar along the vertical direction and another team including also tree thermocouples was used to measure the temperature distribution at a edge position having a 10 mm distance from the central axis along the vertical direction. In both two teams, the vertical distances between the heated surface and the top thermocouples, between the top thermocouples and the middle

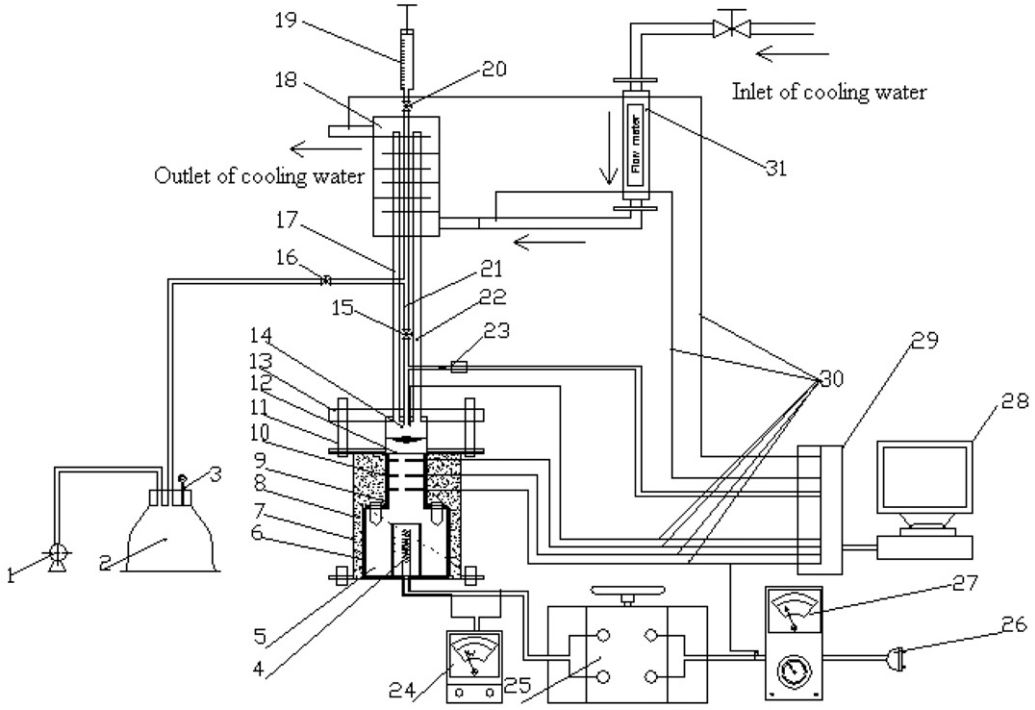

Fig. 1. Schematic of experimental apparatus.

thermocouples and between middle thermocouples and the bottom thermocouples were 4.0 mm, 10 mm and 10 mm, respectively. Besides, other two thermocouples were vertically inserted into the test chamber from the top of condenser to measure the temperatures of bulk liquid and vapor.

It has been confirmed that in the upper column of the copper bar, the temperature distributions of the three temperatures at the centre axial line presented good linear relationship along the vertical direction. Furthermore, at the horizontal direction, the measured temperatures of the two thermocouples at the same level lines were almost equal. While the maximum relative deviation of the wall heat fluxes between the central point and the edge of the heated surface was less than 8%. Therefore, it could be confirmed that the assumption of one-dimensional heat conduction along the vertical direction was well satisfied in the upper column of the copper bar. In order to decrease the system error caused by the thermocouple error and the distance error between the thermocouples, the average wall temperature and the wall heat flux were used in the data management.

The test run was performed under three steady operating pressures of 103 kPa, 20.0 kPa and 7.4 kPa. In each run, the operating pressure was carefully measured and regulated to a set value by controlling the temperature of the cooling deionized water.

In each run, the input power was gradually increased by an increment of 5%. When the measured wall temperature firstly increased abruptly, the power supply was instantly switched off. Then, the run was restarted from the former input power and the power was increased by a 1% increment of the former power. When the measured wall temperatures increased abruptly again, the power supply was instantly switched off and the critical heat flux was recorded. The hysteresis phenomenon has no been measured.

The maximum calibration error of the thermocouple was 0.2 K. The maximum location deviation error between thermocouples was about 1%. The calculated error of the thermal conductivity of the copper bar was estimated as 2%. The measurement error of the power meter was 0.5%. Truncation error of measurement was about 1%. Maximum uncertainties of the heat flux and the heat transfer coefficient were about 9% and 14% respectively.

3. Experimental results and discussions

3.1. The thermoproperties of CNT suspensions

Fig. 4 shows the dependent relation of the viscosity ratio of CNT suspensions on the CNT mass concentration and the liquid temperature. Viscosity ratio was defined as the ratio of the viscosity of the CNT suspension to that of deionized deionized water. The viscosity was measured by an LV DV-II + Brookfield programmable viscometer. It is obvious that the viscosity ratio of CNT suspensions only increases weakly with the increase of the

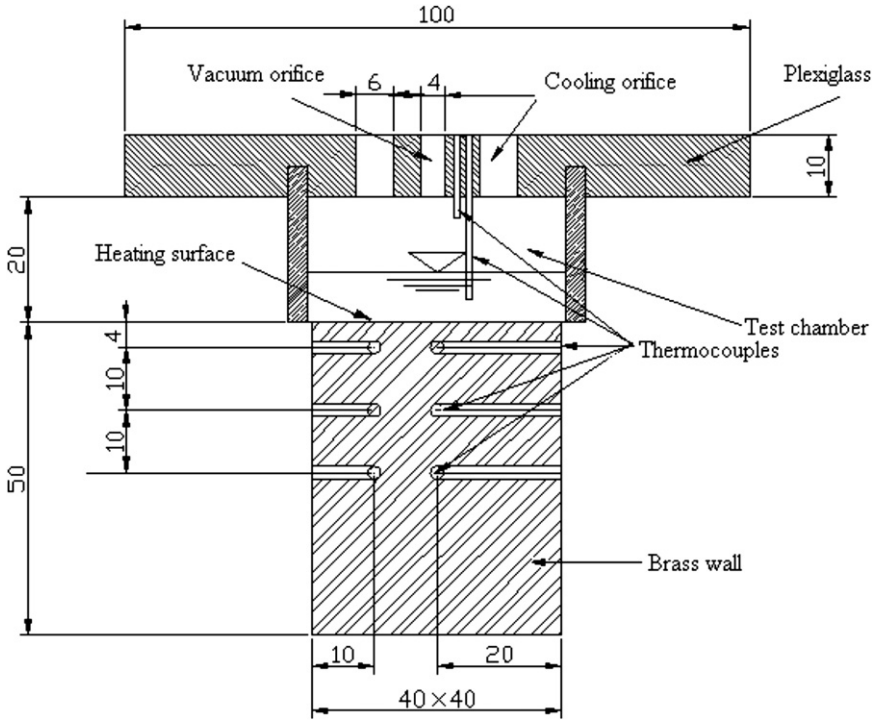

Fig. 2. Schematic of evaporating section (unit: mm).

CNT concentration and has no meaningful changes with varying liquid temperatures.

Fig. 5 shows the thermal conductivity ratio of the CNT suspensions to deionized deionized water. The thermal conductivity was measured by the transient hot wire method. In the present study, the following empirical correlation from the present experimental data may be used for estimating the effective thermal conductivity of CNT suspensions.

$$\frac{\lambda}{\lambda_0} = a_1 \cdot w^2 + a_2 \cdot w \cdot t + a_3 \cdot t^2 + a_4 \cdot w + a_5 \cdot t + a_6 \quad (4)$$

where $a_1 = -2.382$, $a_2 = 0.0227$, $a_3 = 7.255\text{e-}5$, $a_4 = 1.0625$, $a_5 = 2.473\text{e-}4$, $a_6 = 1.0187$. t is the liquid temperature (°C) and w is the mass concentration of CNTs (wt%).

Fig. 6 shows the surface tension ratio of the CNT suspensions to deionized water. It is found that the surface tension ratio reduces rapidly with the increase of CNT mass concentration at low mass concentrations and it trends gradually to a constant at high mass concentrations.

Fig. 7 shows the solid–liquid contact angle of CNT suspensions on both the fresh copper surface and the coated surface after the CNT suspension boiling test with 2.0 wt% CNT concentration at room temperature. The solid–liquid contact angles of the CNT suspension on both the fresh copper surface and the coated surface decrease with the increase of the CNT mass concentration. Then, the contact angles begin to trend the constant values with increasing the mass concentration. While, the contact angles of CNT

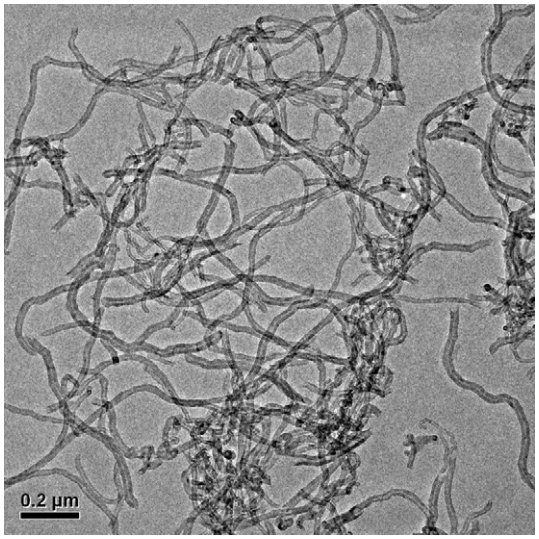

Fig. 3. TEM photograph of carbon nanotube suspension with the mass concentration of 1.0 wt%.

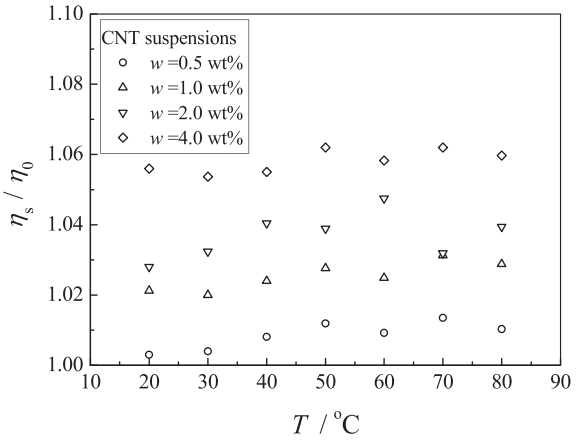

Fig. 4. Viscosity ratio of CNT suspensions.

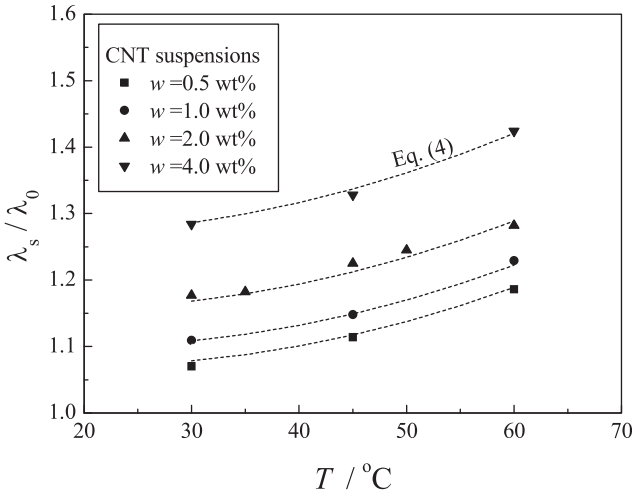

Fig. 5. Thermal conductivity ratio of CNT suspensions.

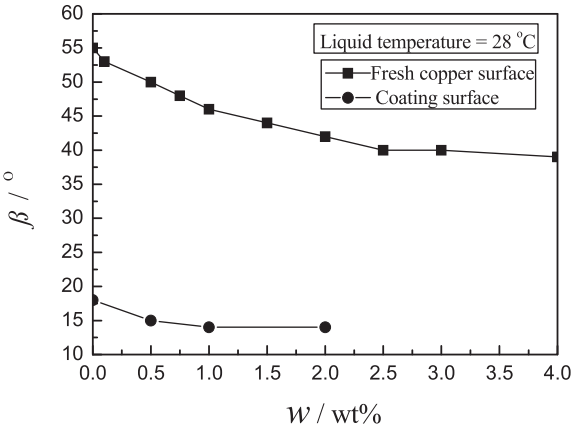

Fig. 7. Solid–liquid contact angle and coated surface of nanofluids on fresh copper surface.

suspensions on the coated surface are apparently lower than that on the copper surface.

3.2. Boiling characteristics of CNT suspensions

Fig. 8 shows the pool boiling curves of deionized water under different pressures on the fresh copper surface. Heat transfer coefficients (HTCs) in the present study are compared with the following equation given by Kutateladze [29].

$$\frac{h}{\lambda}\sqrt{\frac{\sigma}{g(\rho_l-\rho_v)}} = 7.0\times10^{-4}\mathrm{Pr}_l^{0.35} \times\left[\frac{q}{\rho_v h_{\mathrm{fg}}\nu_l}\sqrt{\frac{\sigma}{g(\rho_l-\rho_v)}}\right]^{0.7}\left[\frac{p}{\sigma}\sqrt{\frac{\sigma}{g(\rho_l-\rho_v)}}\right]^{0.7} \quad (5)$$

The critical heat flux (CHF) can be estimated by using the following equation given by Zuber which is widely used to predict the pool boiling CHF for an infinite flat plate heater [30].

$$\frac{q''}{h_{fg}\rho_v^{0.5}[\sigma g(\rho_l-\rho_v)]^{1/4}} = 0.131 \quad (6)$$

If must consider the effect of the contact angle on the CHF, The following empirical equation proposed by Kandlikar [31] as an extension of Eq. (6) may be used. When the contact angle is equal to 57.2°, Eq. (7) and Eq. (6) is the equivalent.

$$\frac{q''}{h_{fg}\rho_v^{0.5}[\sigma g(\rho_l-\rho_v)]^{1/4}} = \left(\frac{1+\cos\beta}{16}\right)\left[\frac{\pi}{4}(1+\cos\beta)+\frac{2}{\pi}\right]^{0.5} \quad (7)$$

It is found the HTCs of deionized water agree reasonably well with Eq. (5) with a maximally relative error of 20%. While, the CHFs of deionized water agree reasonably well with Eqs. (6) and (7) when taking the contact angle as 55° as shown in Fig. 7 with the maximally relative errors of 24% and 23%, respectively. These date firmed creditability of the experimental apparatus.

Fig. 9(a), (b) and (c) show the boiling curves of CNT suspensions at the pressures of 103 kPa, 20.0 kPa and 7.4 kPa, respectively. It is indicated that the mass concentration of CNT suspensions has great influences on the boiling heat transfer for all test pressures. For each pressure, HTC of the CNT suspension increases gradually with the increase of the mass concentration when the concentration is less than 2.0 wt%. Then, the enhancement effect slightly weakens when the mass concentration is over 2.0 wt%. The mass concentration of 2.0 wt% corresponds to the maximum heat transfer enhancement for all test pressures.

The HTC enhancement effect for the CNT mass concentration of 2.0 wt% is shown quantitatively in Fig. 10. The HTC ratio of the CNT suspension is used to indicate the enhancing effect. It is apparent that the pressure has very significant impacts on the HTC

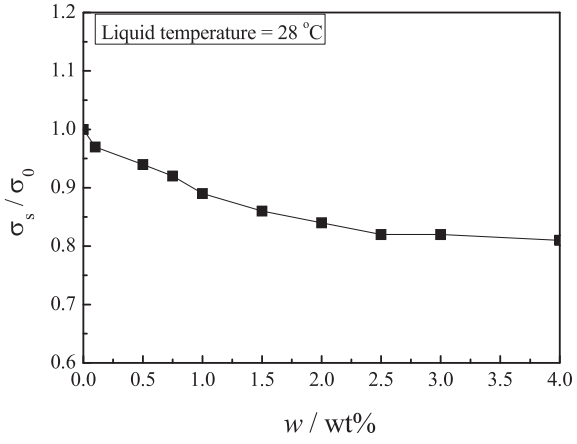

Fig. 6. Surface tension ratio of CNT suspensions.

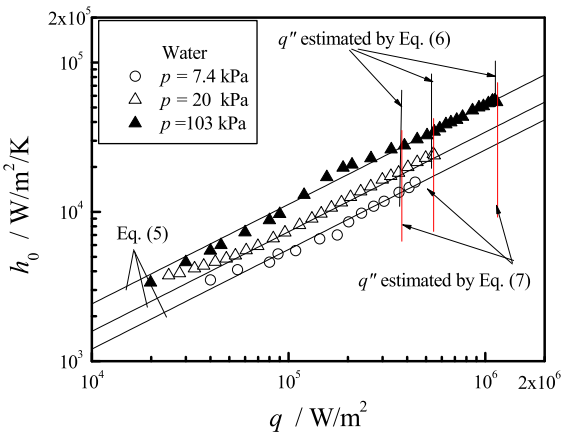

Fig. 8. Boiling curves of deionized water on copper surface at different pressures.

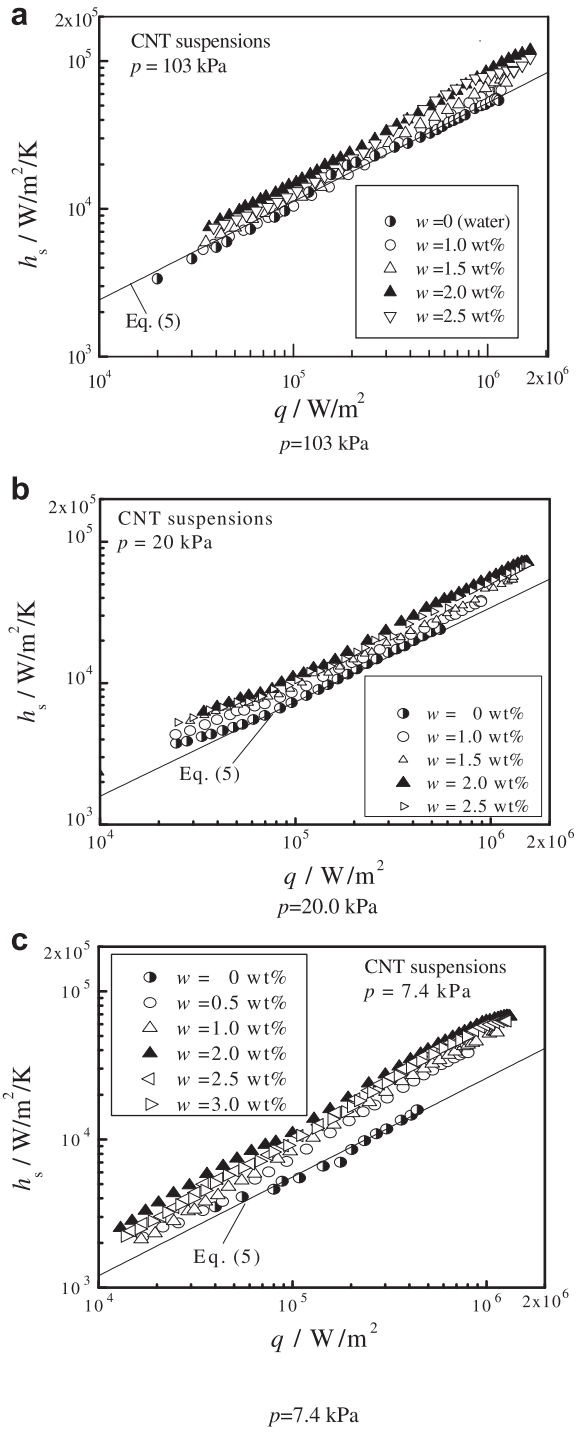

Fig. 9. Boiling curves of CNT suspensions under different pressures.

enhancement ratio and it increases with the decrease of the operating pressure. The HTC can increase maximally by 60% at atmospheric pressure, while 130% at the pressure of 7.4 kPa.

Fig. 11 illustrates the influence of the CNT mass concentration on the CHF ratio of CNT suspensions. The CHF ratio firstly increases with the increase of the CNT mass concentration. Then, it gradually trends to a constant value when the mass concentration is over 2.0 wt%. At atmospheric pressure, the CHF of CNT suspensions can increase by 63%, while by about 200% at the pressure of 7.4 kPa. The CHF enhancement is more significant at sub-atmospheric pressures.

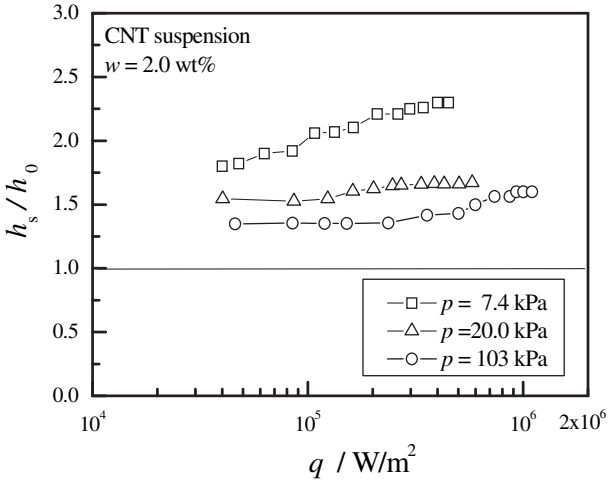

Fig. 10. Heat transfer enhancement ratio of CNT suspension with 2.0 wt% concentration.

In the present study, both the HTC and the CHF are apparently enhanced by adding CNT into deionized water. In especial, the enhancement effect is very significant at sub-atmospheric pressures.

3.3. Effect of the surface characteristics of the heated surface on boiling characteristics of CNT suspensions

Das et al. [15] reported a reduction of the surface roughness after a boiling test using nanoparticle suspensions. Since the size of nanoparticles is one to two orders of magnitude smaller than the roughness of the copper surface, nanoparticles deposited on relatively uneven surface and formed a coated layer during boiling. The decrease of the surface roughness was thought to reduce the boiling heat transfer. Bang and Cheng [17] thought that the CHF was mainly affected by surface characteristics, such as the contact angle. The CHF would increase with the decrease of the contact angle due to the formation of the coated layer on the heated surface. Kim et al. [26–28] considered that the CHF enhancement resulted mainly from the formation of a porous layer by nanoparticles on the heated surface. They established the nexus between CHF enhancement and the surface wettability change, i.e. the contact angle change caused by nanoparticle deposition, and guessed that the mechanism of CHF enhancement in nanofluids was due to the decrease of the contact angle caused by nanoparticle deposition.

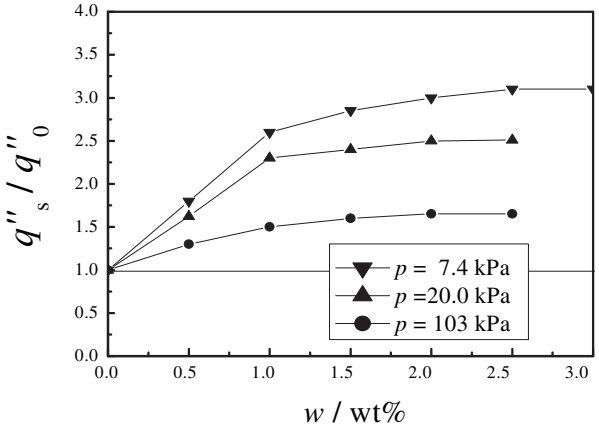

Fig. 11. Effect of mass concentration of nanofluids on CHF enhancement at different pressures.

In the present study, after boiling tests using both deionized water and the CNT suspension, the heated surfaces were directly taken TEM photographs to understand the surface states as shown in Fig. 12 (a) and (b). Then, the heated surface after the CNT suspension boiling was flushed by deionized water to clean out the CNT chips deposited on the heated surface. The heated surface status after a deionized water flushing process was shown in Fig. 12 (c) to compare with the heated surface status without a deionized water flushing process.

It is found that the heated surface was also covered by a loose CNT porous layer consisted of CNT chips after the boiling test. The porous layer can be flushed away by deionized water. However, there still existed a thin coated layer after the flushing process. Contact angles of deionized water and CNT suspensions on the coated surface (before the flushing process) have been illustrated in Fig. 7. Here, the "coated surface" was the heated surface after the boiling test using the CNT suspension with the mass concentration of 2.0 wt% after the boiling time of 6 h.

In this study, the boiling characteristics of deionized water on the coated surface were also carried out and compared with those of CNT suspensions to investigate the effect of solid–liquid contact angle on both the HTC and the CHF on the same coated surface.

Fig. 13(a) and (b) show the comparisons of boiling curves among the water/copper surface, the water/coated surface and the CNT suspension/coated surface. Here, the coated surface used to "the water/coated surface" test was the same coated surface after the boiling test using the CNT suspension.

For atmospheric pressure, the experimental CHF values of deionized water on the copper surface, and the coated surface are 1.14 MW/m^2 and 1.28 MW/m^2, respectively. They agree reasonably well with the calculated values by Eq. (7) if using the data of the contact angles shown in Fig. 7. The experimental CHF value of CNT suspension is 1.68 MW/m^2. It increases by 31% compared with that of deionized water on the coated surface. It may be considered that during deionized water boiled on the coated surface, the coated surface had been cleaned out by deionized water, and then the surface state was different from that of the coated surface during the CNT suspension boiled. Therefore, the boiling characteristics for the two cases were also different. This experimental result shows that the presumption of the CHF enhancement effect resulting from change of the contact angle should be acceptable for atmospheric pressure condition.

For the reduced pressure of 7.4 kPa, the experimental CHF values of deionized water on the copper and the coated surfaces are 0.44 MW/m^2 and 0.52 MW/m^2, respectively. They agree also well with the calculated values by Eq. (7). However, the experimental CHF value of the CNT suspension is 1.32 MW/m^2. It increases about one time compared with that of deionized water on the same coated surface. Therefore, it is unsuitable to explain the CHF enhancement of nanofluids using only change of the contact angle.

In theoretical, the decrease of the contact angle results in the decrease of the heat transfer coefficient at the same surface roughness. However, as shown in Fig. 13, the HTCs of CNT suspensions are apparently higher than those of deionized water on the same coated surface. In particular, the HTCs of CNT suspensions are about 130% higher than those of deionized water on the same coated surface under the reduced pressure of 7.4 kPa. Therefore, the enhancement mechanism of CNT suspensions is more complex than that has been speculated [27–31]. It should also be related to the effects of the accumulation and the disturbing move of CNT in the thin liquid microlayer underneath a vapor bubble on the heated surface [32–35].

According to the dry-spot theory of boiling heat transfer [32–35], the reason why adding nanoparticles into the base liquid could more significantly enhance the boiling heat transfer at the

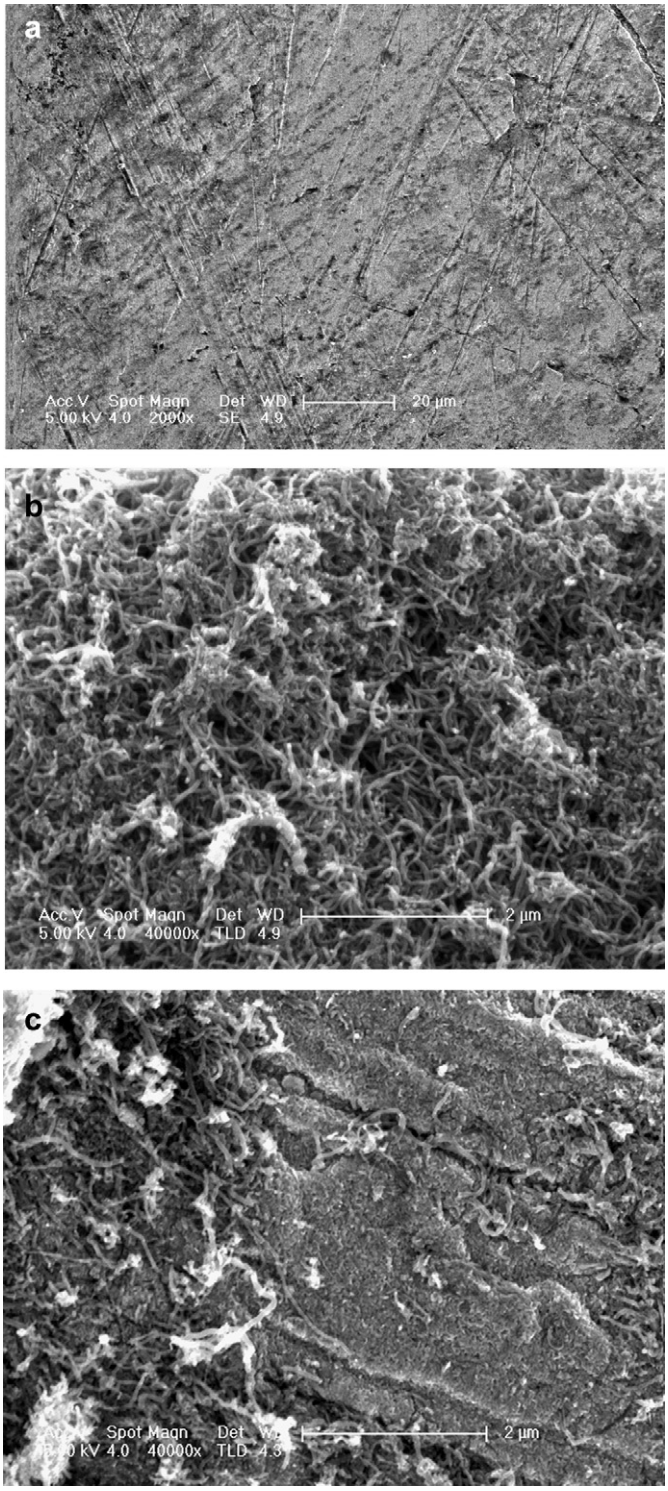

Fig. 12. TEM photographs of the heated surfaces after the boiling tests (a) the heated surface after deionized water boiling test (b) the heated surfaces after the CNT suspension boiling test (c) the heated surface after the CNT suspension boiling test and the flushing process.

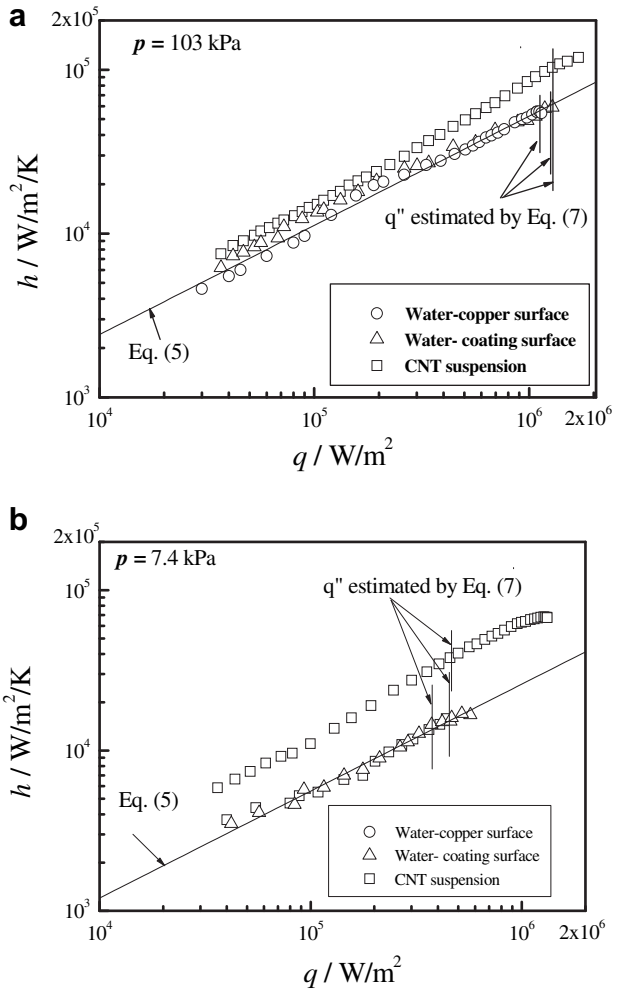

Fig. 13. Effect of the heated surface state on the heat transfer characteristics (a) atmospheric pressure; (b) sub-atmospheric pressure.

sub-atmospheric pressures may be guessed as the following. Both the HTC and the CHF of pool nucleate boiling depend on the thickness and the wettability area of the thin liquid microlayer underneath vapor bubbles. If the CNT nanoparticles accumulated in the liquid microlayer during the boiling process, both the HTC and the CHF can be increased due to that the increases of both the effective thermal conductivity and the wettability area of the thin liquid microlayer. In the atmospheric pressure, the effects of the accumulation of CNTs in the thin liquid microlayer may be weak due to that it is difficult for nanoparticles to enter into the liquid microlayer. However, in the sub-atmospheric pressures, the effects of the accumulation may be stronger than that in the atmospheric pressure, so the heat transfer enhancement would increase with the decrease of the pressure.

The reason why there exists an optimal nanoparticle mass concentration corresponding to the best heat transfer enhancement may be explained as below. The changes of the boiling heat transfer of CNT suspensions on the same heated surface should result from two influencing factors. One is the effect caused by the changes of thermoproperties of CNT suspensions as shown in Figs. 4–7. The other is the effects caused by the accumulation and the disturbing move of CNT in the liquid microlayer. According to Eq. (5), the first factor would cause the decrease of the HTC. And according to the dry-spot theory of the boiling heat transfer, the second factor would cause the increase of the HTC. As the increase of CNT mass concentration, the effect from the first one would reduce and the effect from the second one would increase. At a balance point, an optimal mass concentration would exist which corresponds to the maximum heat transfer enhancement.

The explanations mentioned above are only some qualitative presumptions. We would carry out a numeral simulation according to dry-spot theory in the next study step.

4. Conclusion

An experimental study was performed to investigate the pool boiling heat transfer of water-based carbon nanotube (CNT) suspensions. The following results are obtained:

1. The pressure has significant influences on both the HTC enhancement and CHF enhancement of CNT suspensions. They all increase apparently with the decrease of the pressure. At atmospheric pressure, the HTC and the CHF of CNT suspensions can increase by about 60% and 63% respectively. At the sub-atmospheric pressure of 7.4 kPa, however, they can increase by about 130% and 200% compared with those of deionized water.
2. The mass concentration of CNT suspensions has strong impacts on both the HTC and the CHF of CNT suspensions. The CNT mass concentration of 2.0 wt% corresponds to the maximum heat transfer enhancement for all test pressures.
3. Both the HTC and the CHF of CNT suspensions are much higher than those of deionized water on the same coated surface at sub-atmospheric pressure. The solid–liquid contact angle or the surface characteristics of the heated surface is not sole influencing factor to enhance heat transfer of CNT suspensions.

References

[1] S.U.S. Choi, Enhancing thermal conductivity of fluids with nanoparticles, in: Proceedings of the 1995 ASME International Mechanical Engineering Congress and Exhibition, 1995, San Francisco, CA, USA.
[2] S. Lee, S.U.S. Choi, S. Li, J.A. Eastman, Measuring thermal conductivity of fluids containing oxide nanoparticles. ASME Journal of Heat Transfer 121 (1999) 280–289.
[3] J.A. Eastman, S.U.S. Choi, S. Li, W. Yu, Anomalously increasing effective thermal conductivities of ethylene glycol-based nanofluids containing copper nanoparticles. Applied Physics Letter 78 (2001) 718–720.
[4] B.X. Wang, L.P. Zhou, X.P. Peng, A fractal model for predicting the effective thermal conductivity of liquid with suspension of nanoparticles. International Journal of Heat and Mass Transfer 46 (2003) 2665–2672.
[5] D.S. Wen, Y.L. Ding, Effective thermal conductivity of aqueous suspensions of carbon nanotubes (nanofluids). Journal of Thermophysics and Heat Transfer 18 (2004) 481–485.
[6] S.K. Das, N. Putra, W. Roetzel, Temperature dependence of thermal conductivity enhancement for nanofluids. Journal of Heat Transfer 125 (2003) 567–574.
[7] S. Lee, S.U.S. Choi, Application of metallic nanoparticle suspensions in advanced cooling systems, in: Proceedings of International Mechanical Engineering Congress and Exhibition, 1996, Atlanta, USA
[8] K.B. Pak, Y.I. Cho, Hydrodynamic and heat transfer study of dispersed fluids with submicron metallic oxide particles. Experimental Heat Transfer 11 (1999) 151–170.
[9] Y.M. Xuan, Q. Li, Heat transfer enhancement of nanofluids. International Journal of Heat and Fluid Flow 21 (2000) 58–64.
[10] D.S. Wen, Y.L. Ding, Experimental investigation into convective heat transfer of nanofluids at the entrance region under laminar flow conditions. International Journal of Heat and Mass Transfer 47 (2004) 5181–5188.
[11] G. Roy, W. Nguyen, S.K. Das, Numerical investigation of laminar flow and heat transfer in a radial flow cooling system with the use of nanofluids. Superlattices and Microstructures 35 (2003) 497–511.
[12] S.E.B. Maiga, C.T. Nguyen, N. Galanis, G. Roy, Heat transfer behaviors of nanofluids in a uniformly heated tube. Superlattices and Microstructures 26 (2004) 543–557.
[13] Y. Yang, Z. Zhang, E. Grulke, W. Anderson, G. Wu, Heat transfer properties of nanoparticles-in-fluid dispersions (nanofluids) in laminar flow. International Journal of Heat and Mass Transfer 48 (2005) 1107–1116.
[14] L. Lee, I. Mudawar, Assessment of the effectiveness of nanofluids for single-phase and two-phase heat transfer in micro-channels. International Journal of Heat and Mass Transfer 50 (2007) 452–463.

[15] S.K. Das, N. Putra, W. Roetzel, Pool boiling characteristics of nanofluids. International Journal of Heat and Mass Transfer 46 (2003) 851–862.
[16] P. Vassallo, R. Kuman, S.D. Amico, Pool boiling heat transfer experiments in silica-deionized water nano-fluids. International Journal of Heat and Mass Transfer 47 (2004) 407–411.
[17] I.C. Bang, S.H. Chang, Boiling heat transfer performance and phenomena of Al_2O_3-deionized water nanofluids from a plain surface in a pool. International Journal of Heat and Mass Transfer 48 (2005) 2407–2419.
[18] D.S. Wen, Y.L. Ding, Experimental investigation into the pool boiling heat transfer of aqueous based alumina nanofluids. Journal of Nanoparticles Research 7 (2005) 265–275.
[19] S.M. You, J.H. Kim, K.H. Kim, Effect of nanoparticles on critical heat flux of deionized water in pool boiling heat transfer. Applied Physics Letters 83 (2003) 3374–3376.
[20] S.K. Das, N. Putra, W. Roetzel, Pool boiling of nano-fluids on horizontal narrow tubes. International Journal of Multiphase Flow 29 (2003) 1237–1247.
[21] Z.H. Liu, L. Liao, Sorption and agglutination phenomenon of nanofluids on a plane heated surface during pool boiling. International Journal of Heat and Mass Transfer 51 (2008) 2593–2601.
[22] Z.H. Liu, X.F. Yang, G.L. Guo, Effect of nanoparticles in nanofluid on thermal performance in a miniature thermosyphon. Journal of Applied Physics 102 (1) (2007) 13–26.
[23] Z.H. Liu, Y.H. Qiu, Boiling heat transfer characteristics of nanofluids jet impingement on a plate surface. Heat Mass Transfer 43 (2007) 699–706.
[24] K. Park, H.B. Ma, Nanofluid effect on heat transport capability in a well-balanced oscillating heat pipe. Journal of Thermophysics and Heat Transfer 21 (2007) 443–445.
[25] S.J. Kim, T. Mckrell, I.C. Bang, J. Buongiorno, L.W. Hu, Alumina nanoparticles enhance the flow boiling critical heat flux of deionized water at low pressure. Journal of Heat Transfer 130 (2008) 044501.
[26] S.K. Das, G.P. Narayan, K.B. Anoop, Survey on nucleate pool boiling of nano-fluids: the effect of particle size relative to roughness. Journal of Nanoparticle Research 10 (2008) 1099–1108.
[27] G.P. Narayan, K.B. Anoop, G. Sateesh, S.K. Das, Effect of surface orientation interaction on pool boiling heat transfer of nanoparticle suspensions. International Journal of Multiphase Flow 34 (2008) 145–160.
[28] G.P. Narayan, K.B. Anoop, S.K. Das, Mechanism of enhancement/deterioration of boiling heat transfer using stable nanoparticle suspensions over vertical tubes. Journal of Applied Physics 102 (2007) 074317.
[29] S.J. Kim, I.C. Bang, J. Buongiorno, L.W. Hu, Effects of nanoparticle deposition on surface wettability-influencing boiling heat transfer in nanofluids. Applied Physics Letter 89 (2006) 153107.
[30] S.J. Kim, I.C. Bang, J. Buongiorno, L.W. Hu, Surface wettability change during pool boiling of nanofluids and its effect on critical heat flux. International Journal of Heat and Mass Transfer 50 (2007) 4105–4116.
[31] H. Kim, M. Kim, Experimental study of the characteristics and mechanism of pool boiling CHF enhancement using nanofluids. Heat Mass Transfer 45 (2009) 991–998.
[32] S.S. Kutateladze, A hydrodynamic theory of changes in the boiling process under free convection conditions, Isv. Akad Nauk, USSR, Otd Tekh Nauk 4 (1951) 529–935.
[33] N. Zuber, On the stability of boiling heat transfer. ASME Journal of Heat Transfer 80 (1958) 711–720.
[34] S.J. Kandlikar, A theoretical model to predict pool boiling CHF incorporating effects of contact angle and orientation. Journal of Heat Transfer 123 (2001) 1071–1079.
[35] O. Toshihako, A. Yoshiyuki, H. Yasuhiko, A. Nagashima, Pool boiling heat transfer in microgravity. JSME International Journal Series B 39 (1) (1996) 23–27.